Power Amplification of Microwave FM Communication Signals Using a Phase-Locked Voltage-Tuned Oscillator

MARION E. HINES, FELLOW, IEEE, RONALD S. POSNER, MEMBER, IEEE, AND ALLEN A. SWEET, MEMBER, IEEE

Abstract—**An analog phase-locked oscillator is used as a power amplifier for FM communications signals. Intended service is for FDM telephone message service or television relay. The output power is generated in a varactor-tuned oscillator, which is synchronized with a weak input signal using a phase-lock loop. This involves a phase detector and a wide-band direct-coupled video amplifier whose output is applied to the tuning varactor.**

The paper is largely theoretical, relating the parameters of the feedback loop to the performance of the overall device. Explicit expressions are derived for the noise figure, the frequency response of the modulation characteristic, AM–PM conversion, and nonlinearity effects in terms of differential gain and intermodulation. In addition, two experimental models are described, together with certain measured data.

The phase-lock method differs in many ways from multistage reflection amplifiers and appears to offer advantages for many applications. The device has adequate bandwidth and linearity for a single FDM–FM signal with 1800 or more channels, but must be tuned to the intended frequency. Tuning procedures are simple.

High gain of 25–35 dB is obtainable in a single microwave "stage." Most of this gain may be associated with the functions of phase detection, video amplification, and VCO tuning. Of major importance, with respect to noise, is that the device is functionally equivalent to a high-gain low-noise microwave preamplifier followed by a low-gain power amplifier stage in which the preamplifier has the noise figure of the phase detector combined with the video amplifier, and the power stage has a noise figure appropriate to the class of power diode used. FM noise generation is substantially lower than in a high-gain reflection amplifier using the same class of microwave power diode throughout.

I. Introduction

THIS PAPER describes the application of a phase-lock loop to provide power amplification of microwave FM communication signals. The device is intended to serve as the transmitting amplifier for microwave radio-relay communication links for multiplex telephone message service and television. An experimental amplifier is described, together with the test data applicable to such service. The paper is largely theoretical, however, presenting an analysis of the relationships of the internal parameters of the phase-lock loop to the system performance expected.

In our experimental amplifier, a 2-mW input signal is adequate to obtain a power output of 250 mW at 11 GHz, using a Gunn oscillator. Using an IMPATT diode oscillator, a power output of 3 W has been obtained. Future extension to higher power appears to be feasible with multiple IMPATT diodes. These are "single-stage" devices in that only one microwave power source is used. Lower frequency transistors are used in the video amplifier in the feed-back loop.

The phase-lock loop uses a varactor-tuned voltage-controlled oscillator (VCO) as the source of microwave power. As indicated in Fig. 1, the loop also includes a Schottky-barrier-diode balanced mixer acting as a phase detector, and a wide-band direct-coupled transistor video amplifier. With an input microwave FM signal, wide-band phase lock of the power oscillator is obtained and the output oscillator closely follows the frequency deviations of the input signal. A small sample of the oscillator's output is fed back to the phase detector. This generates an error signal at video frequencies which is amplified and used to tune the oscillator. Feedback maintains the phase error at a small value.

At present, traveling-wave tubes are most widely used for power amplification for frequencies of 6 GHz and above. For reasons of cost and reliability, a solid-state replacement is being sought in many laboratories. Commercially available amplifying devices for powers of 1–10 W include only Gunn and IMPATT negative-resistance diodes. The most widely studied circuits are circulator-coupled reflection amplifiers, which may be of the stable variety or may involve an injection-locked oscillator. Although much progress has been made with these devices [1], [2], the results are not entirely satisfactory. For a high gain, complex multistage circuits are needed and the noise performance with IMPATT diodes is a serious problem. Other problems include AM–PM conversion and, in some cases, spurious signals may be generated at high power levels.

In our laboratory we have been seeking a viable alternative. Theoretical and experimental studies with the phase-lock principle have led us to believe that it is a superior approach for many of the intended applications, compared with a reflection amplifier. Its advantages may include adequate total gain in a single stage, a highly satisfactory noise figure, adequate linearity and bandwidth, and improved overall efficiency. Tests indicate that the noise and linearity are suitable for 1800 channel FDM telephone message service in long-haul multihop systems. Unlike the

Manuscript received June 13, 1975; revised January 19, 1976.

M. E. Hines and R. S. Posner are with Microwave Associates, Inc., Burlington, MA 01803.

A. A. Sweet was with Microwave Associates, Inc., Burlington, MA 01803. He is now with Varian Associates, Palo Alto, CA.

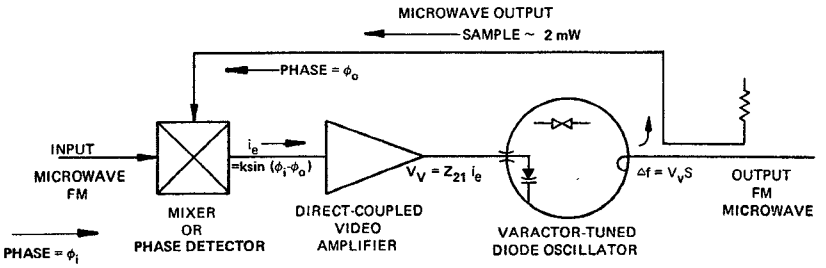

Fig. 1. Block diagram of dynamic phase-lock power amplifier for FM signals, with parameters for linear analysis.

traveling-wave tube, the phase-lock device must be tuned to the intended frequency. This is easily accomplished with simple instrumentation.

The objectives of this paper are 1) to present a theoretical treatment of the device which relates the performance for FM communications to the internal parameters of the phase-lock loop, and 2) to present some experimental data which illustrate the applicability of the method. No attempt is made to justify its "superiority" over other amplification methods.

Phase-locked loops are widely used in instrumentation, in frequency synthesizers, in receiver demodulators, and in stabilized low-noise local oscillators. For these applications, the principles are well understood. In a recent review, Gupta [3] summarizes the state-of-the-art and provides a bibliography of 188 publications. Klapper and Frankle [4] provide a comprehensive text with a larger bibliography. For application as a microwave power amplifier, however, the phase-lock technique is less well known. It has been used in commercial radio equipment [5] in which the output-signal power is generated by a transistor power amplifier and a varactor frequency multiplier which is incorporated into the loop. A recent report by Salmon [6] describes an X-band IMPATT-diode phase-locked oscillator whose principles are quite similar to the device reported here.

In its basic principles this phase-lock loop is conventional. However, it differs from most earlier devices in that it uses a very broad-band feedback loop in order to obtain high-fidelity transmission of wide-band communication signals. The analysis is concerned with the relationships of the internal loop parameters to the system performance. We are concerned with the frequency response of the modulation, with the linearity as it affects intermodulation and other distortions, with AM–PM conversion, and with FM noise generation. These system parameters are presented in the terms commonly used by communications system engineers.

II. Loop Analysis

A. Basic Equations

The phase-lock loop of Fig. 1 serves as a power amplifier for FM signals. The purpose of this analysis is to determine the effects of the system parameters on the fidelity of the response, particularly in the transmission of the information content as carried by the frequency modulation. Amplitude modulation on the input may be present due to distortions in previous stages. This is undesirable and its effects should be minimized. We will be concerned with how incidental AM affects the FM response.

The input frequency deviation $\tilde{f}_i(t)$ is a time function[1] which has a direct proportional correspondence with the baseband message signal being carried. The spectrum of $\tilde{f}_i$ extends from near zero frequency to ~8 MHz, typically. The input carrier wave can be described as a modulated sinusoidal function

$$v_i = v_{ic}(t) \cos \left[\varphi_i(0) + 2\pi \int_0^t (\tilde{f}_i(\tau) + f_c)\, d\tau\right] = v_{ic}(t) \cos \varphi_i(t) \tag{1a}$$

where f_c is the carrier frequency, and $\varphi_i(t)$ is the "instantaneous phase" of the input carrier. If phase lock is maintained, the output wave is similar

$$v_o = v_{oc}(t) \cos \left[\varphi_o(0) + 2\pi \int_0^t (\tilde{f}_o(\tau) + f_c)\, d\tau\right] = v_{oc}(t) \cos \varphi_o(t). \tag{1b}$$

The carrier amplitudes are here shown to be variable, although this is undesirable in an FM system. The effects of such AM will be studied later.

The mixer phase-detector is assumed to be a square-law device for purposes of analytic ease. In practice, high-level mixers may behave quite differently. With applied carriers as in (1a) and (1b) the rectified video output is presumed to have the well-known form

$$i_e = p v_{ic}(t) v_{oc}(t) \sin [\varphi_i(t) - \varphi_o(t)] \tag{2}$$

where p is a constant related to the conversion loss of the device as a mixer. In the analysis of this section, v_{ic} and v_{oc} are assumed to be constant and the mixer output has the form

$$i_e = k \sin [\varphi_i(t) - \varphi_o(t)] = k \sin \varphi_e(t). \tag{3}$$

The video amplifier is characterized by its complex transfer impedance $Z_{21}(\omega_m)$ which relates the voltage at the varactor to its input current i_e. The video amplifier also includes a dc offset voltage such that the varactor bias will lie ap-

[1] The tilde (~) is used to distinguish frequency deviations from time-sinusoidal frequencies which are not so designated.

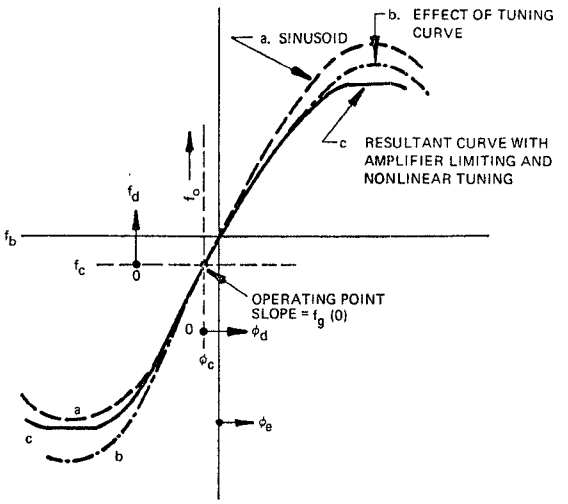

Fig. 2. Sketch showing nonlinearity in the static tuning curve f_o vs. φ_e. f and φ_d excursions about the operating point are small in normal operation, sufficient to provide the frequency modulation needed.

proximately midway within its useful range when the input current i_e is zero. In our device, a very wide-band video amplifier is used which has an essentially flat response from zero up to frequencies far beyond the useful band of video frequencies, preferably to 200 MHz or more.

The VCO has a significantly nonlinear tuning curve, and the video amplifier is also nonlinear. It is helpful to obtain a plot as sketched in Fig. 2 which relates the frequency of the VCO to the static phase difference φ_e at the mixer when it is activated at its microwave ports by two *unmodulated* waves of identical frequency. This curve combines the nonlinearities of the sinusoidal mixer, the video amplifier, and of the VCO tuning curve. The oscillator is to be mechanically tuned so that its frequency is equal to the carrier frequency in the middle range, preferably at or near the point of inflection where it is most nearly linear. At this optimum operating point, the net phase error $\varphi_e = \varphi_c$, a constant. About this point (φ_c, f_c) a power series is assumed to represent the nonlinear static response over the normal FM deviation range

$$f_o = f_c + f_g(0)(\varphi_d + r_2\varphi_d^2 + r_3\varphi_d^3 \cdots) \tag{4}$$

$$\varphi_d = \varphi_i - \varphi_o - \varphi_c = \varphi_e - \varphi_c \tag{5}$$

where $f_g(0)$ is the slope of the curve at the operating point. As written in (4), $f_g(0)$ is the effective forward gain at dc, a constant. For small-signal ac excitation in a *linear* analysis, $f_g(\omega_m)$ is the complex transfer characteristic relating the output frequency deviation $\tilde{f}_o$ to the phase deviation φ_d at the mixer when $\varphi_d(t)$ is a sinusoid varying at the frequency ω_m. This is given by

$$f_g(\omega_m) = kZ_{21}(\omega_m)S \quad \text{(Hz/rad)} \tag{6}$$

where S is the deviation sensitivity of the VCO at the operating point, given in hertz per volt. The quantity f_g is a critical parameter of the system. It is called the "characteristic frequency." As a representation of the feedback-loop gain, a large value for f_g is helpful in obtaining linear operation with nonlinear components in much the same way as in other feedback amplifiers.

B. Linear Analysis

For small deviations such that $\varphi_d \ll 1$, the tuning equation of (4) may be linearized by ignoring the terms in φ_d^2 and φ_d^3. In (6) $Z_{21}(\omega_m)$ is assumed to include all delay and band-limiting elements in the mixer output, in the video amplification, and in the varactor input choke of the VCO. As indicated in unpublished work, the frequency deviation response of the VCO is substantially uniform with frequency with negligible delay. In the transmission path back from the VCO to the mixer, an additional simple delay is included of τ_b s. Thus, for a sinusoidal variation in the phase angle φ_d, the frequency returned to the mixer is given by

$$\begin{aligned} f_o(t) &= f_c + f_g(\omega_m)e^{-j\omega_m\tau_b}\varphi_d e^{j\omega_m t} \\ &= f_c + \tilde{f}_o(t). \end{aligned} \tag{7}$$

In the three steps of (8) below, (5) is first differentiated, then (7) is substituted to obtain the basic loop equation.

$$\begin{aligned} \frac{d\varphi_d}{dt} &= \frac{d\varphi_i}{dt} - \frac{d\varphi_o}{dt} \\ j\omega_m\varphi_d &= 2\pi\tilde{f}_i(t) - 2\pi\tilde{f}_o(t) \\ j\omega_m\varphi_d &= 2\pi\tilde{f}_i(t) - 2\pi f_g(\omega_m)e^{-j\omega_m\tau_b}\varphi_d \end{aligned} \tag{8}$$

whose steady-state solution is

$$\varphi_d = \frac{2\pi\tilde{f}_i}{j\omega_m + 2\pi f_g(\omega_m)e^{-j\omega_m\tau_b}}. \tag{9}$$

Again using (7) we obtain the complex transmission coefficient (as seen at the mixer's feedback port) $T_{fm}(\omega_m)$ for an input frequency deviation which is sinusoidal at the

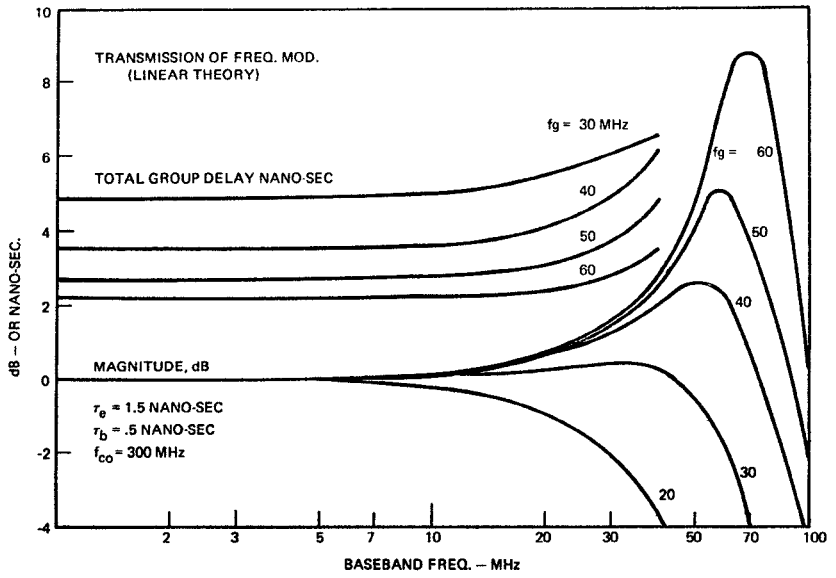

Fig. 3. Theoretical response of the frequency modulation of an FM phase-lock amplifier for a particular set of parameters. Loop gain is proportional to the parameter f_g.

frequency f_m

$$T_{\text{fm}}(\omega_m) = \frac{\tilde{f}_o}{\tilde{f}_i} = \frac{\dfrac{2\pi f_g(\omega_m)e^{-j\omega_m\tau_b}}{j\omega_m}}{1 + \dfrac{2\pi f_g(\omega_m)e^{-j\omega_m\tau_b}}{j\omega_m}}. \tag{10}$$

It can easily be shown that the ratio of this closed-loop response to the open-loop response is given as K_s

$$K_s = \frac{1}{1 + \dfrac{2\pi f_g(\omega_m)e^{-j\omega_m\tau_b}}{j\omega_m}}. \tag{11}$$

This is a "suppression factor" which applies to the effects of noise and small nonlinear distortions which may appear anywhere in the loop. Use will be made of this formula in the section on FM noise. The factor $2\pi f_g(\omega_m)e^{-j\omega_m\tau_b}/j\omega_m$ is the "open-loop gain" of the system. Stability of the loop can be analyzed in the usual manner with a Nyquist diagram. In most cases, the circuit will be stable if this quantity has a magnitude less than 1.0 at the frequency where its phase lag is π rad.

To illustrate the behavior of a typical system, similar to that used in our experiments, we have made computations for (10) and (11) assuming that $Z_{21}(\omega_m)$ has the behavior of two tandem stages with simple *RC*-type cutoff characteristics. We have also added excess flat delay of τ_e s. The open-loop gain expression then assumes the form on the right side of (12)

$$\frac{2\pi f_g(\omega_m)e^{-j\omega_m\tau_b}}{j\omega_m} \rightarrow \frac{2\pi f_g(0)e^{-j\omega_m(\tau_e+\tau_b)}}{j\omega_m\left(1 + j\dfrac{\omega_m}{2\pi f_{co}}\right)^2} \tag{12}$$

where f_{co} is the 3-dB bandwidth of each of the two amplifier stages. Fig. 3 shows plots of the transfer function T_{fm} (as seen at the oscillator[2]) for $\tau_e = 1.5$ ns, $\tau_b = 0.5$ ns, and $f_{co} = 300$ MHz, with various values of the characteristic frequency $f_g(0)$, from 20 to 60 MHz/rad. As the gain is increased, a peaking effect is found to occur between 40 and 100 MHz. If the gain $f_g(0)$ were increased to 109 MHz/rad, it is predicted that the loop would oscillate at a frequency above 100 MHz. The effects of excess delay are shown in Fig. 4. Here we fix the characteristic frequency at 50 MHz/rad and show plots for various values of excess delay.

Fig. 5 shows plots of the suppression factor K_s for the same conditions as in Fig. 3.

III. Nonlinear Distortion

A. General Discussion

In this section, we derive expressions for various distortion characteristics in the form familiar to the designers of FM communication equipment. These include "differential gain," "differential phase," or "differential delay," intermodulation effects, and AM–PM conversion. These quantities and their measurement techniques are described in [7].

We are primarily concerned with the transmission of FDM telephone message service where 1800 or more channels may be transmitted. The baseband signal is an array of single-sideband up-converted telephone signals, distributed over the baseband up to ~8 MHz in an 1800-channel system. For this service, the frequency response, as plotted in Fig. 3, is important in maintaining uniform signal strength for the multiple channels. Nonlinear dis-

[2] In Fig. 3 the curves for delay in transmission are taken at the oscillator. T_{fm} elsewhere in this paper applies to the output as seen at the feedback port of the mixer. The only difference is the simple delay τ_b s.

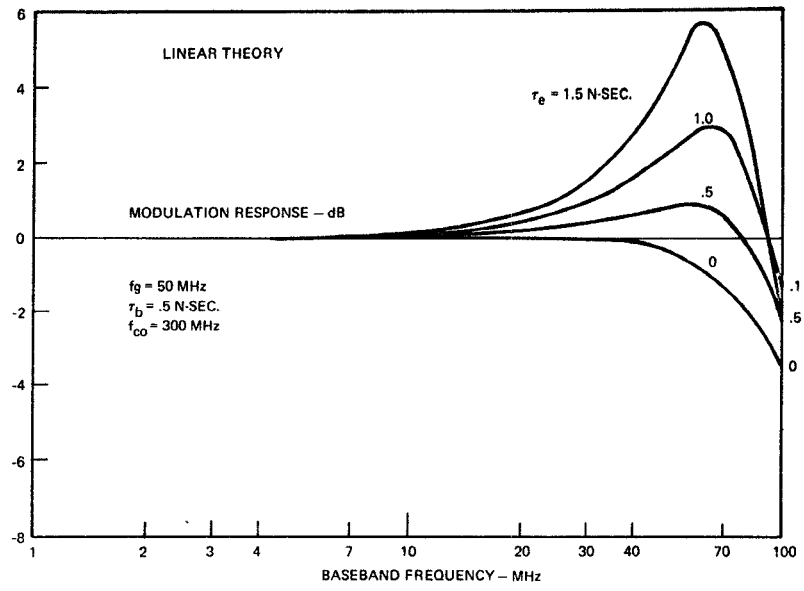

Fig. 4. Effect on the transmission of increased delay in the feedback loop, for the case f_g = 50 MHz/rad.

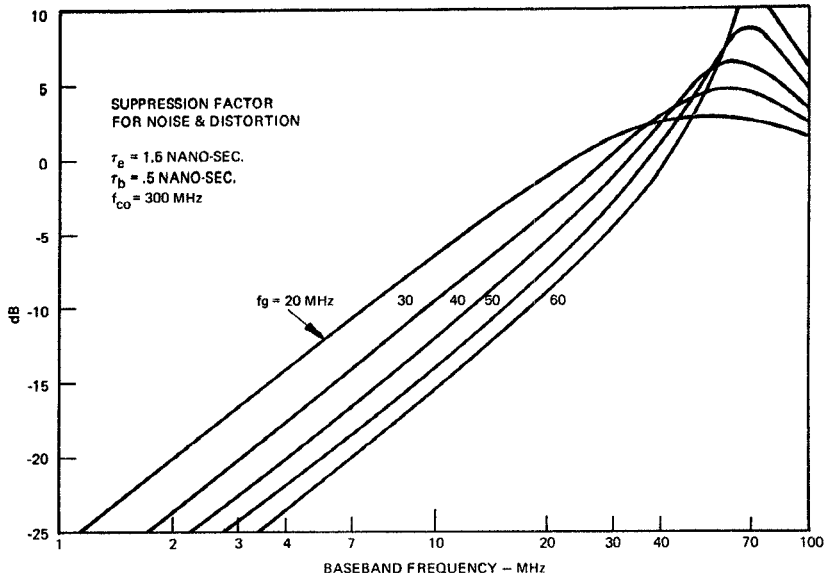

Fig. 5. Theoretical feedback-suppression factor affecting oscillator noise and distortion products generated in the loop.

tortion causes crosstalk between the different channels because of intermodulation. When large numbers of channels are used, crosstalk has the characteristics of noise.

B. Differential Gain and Differential Delay

In evaluating a communication link, one common measurement involves a test signal consisting of a low-frequency wide-deviation (sweeping) modulation plus a superimposed higher frequency deviation of small amplitude. In a test instrument called a "link analyzer" the variations in the transmission gain for the high-frequency signal are measured as a function of the instantaneous deviation of the low-frequency signal. The results are displayed on an oscillograph where the x axis is the sweeping frequency deviation and the y axis is the magnitude of the response for the higher frequency modulating signal. This is the differential gain. Also plotted by this instrument is the differential delay where measurements of the variations in phase for the high-frequency signal are presented as "delay" in nanoseconds. Typical oscillographic displays of this type are shown in Figs. 6 and 7.

In link-analyzer measurements, the operating point may be assumed to vary slowly with time. On the curve of Fig. 2, we may consider that f_c moves up and down the curve. The parameter which changes is the slope of the curve, which causes the magnitude of f_g to vary. It is assumed that no changes in phase occur in f_g. (Some phase changes may, in reality, occur because of the variations in the current being

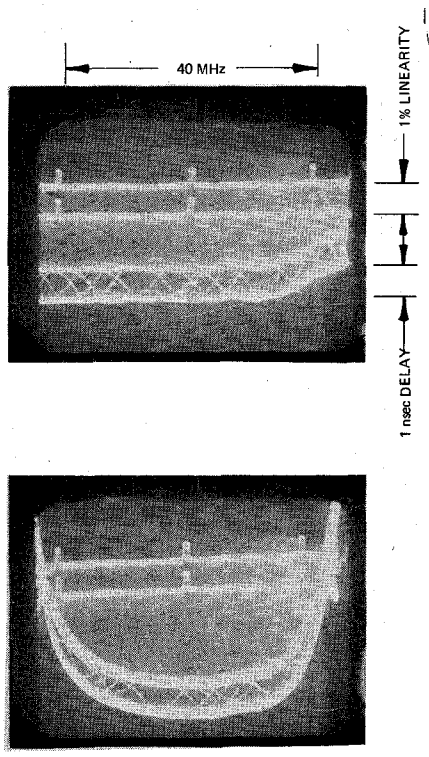

Fig. 6. Link-analyzer test data for the 250-mW Gunn-type phase-lock amplifier. Upper curves show differential gain variation, the lower curves are differential delay. Calibration is determined by the curve separation, representing 1 percent for the gain and 1 ns for the delay. The markers are at 20 MHz above and 20 MHz below band center and the total sweep range is ~50 MHz. The upper photo is for 2-mW input, the lower for 0.5-mW input.

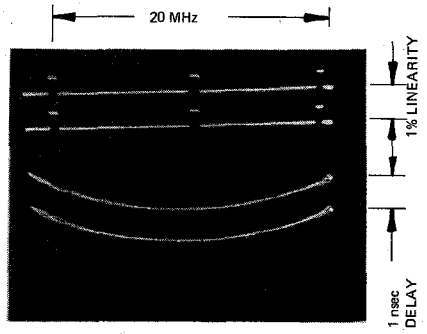

Fig. 7. Link-analyzer test data for a preliminary model using a 3-W IMPATT VCO. In this early model, the VCO has inferior tuning capability, compared with the Gunn device of Fig. 6, resulting in poorer linearity, reduced deviation capability, and a higher noise level. The frequency markers in this case are at ±10 MHz.

drawn by the transistors in the video amplifier.) In practice, the total deviation due to modulation is a small fraction of the total available deviation. Within this narrow range the curve is *nearly* linear.

From (9), for a low frequency, we see that $\varphi_d \approx \tilde{f}_i/f_g$. Differentiating (4), we obtain the approximate result

$$f_g(\varphi_d) = \frac{df_o}{d\varphi_d} = f_g(0)(1 + 2r_2\varphi_d + 3r_3\varphi_d^2 \cdots)$$

$$f_g(\tilde{f}_s) \simeq f_g(0)\left(1 + 2r_2\frac{\tilde{f}_s}{f_g(0)} + 3r_3\frac{\tilde{f}_s^2}{f_g^2(0)}\cdots\right) \quad (13)$$

where $\tilde{f}_s$ is the sweep deviation of the test. The desired result may be obtained by substituting (13) into (10). If f_t is the higher frequency in the test, the result is

$$T_{fm}(f_t,\tilde{f}_s) = \frac{1}{1 + \dfrac{jf_t}{f_g(\omega_t)e^{-j\omega_t\tau_b}\left(1 + r_2\dfrac{\tilde{f}_s}{f_g(0)} + r_3\dfrac{\tilde{f}_s^2}{f_g^2(0)}\right)}}. \quad (14)$$

We are interested in the "differential transmission," $DT = T_{fm}(f_t,\tilde{f}_s) - T_{fm}(f_t,0)$. If the higher order terms in the power series are very small compared with 1, this may be approximated as

$$DT = \frac{jf_t\left(r_2\dfrac{\tilde{f}_s}{f_g(0)} + r_3\dfrac{\tilde{f}_s^2}{f_g^2(0)}\right)}{f_g(\omega_t)e^{-j\omega_t\tau_b}\left(1 + \dfrac{jf_t}{f_g(\omega_t)e^{-j\omega_t\tau_b}}\right)^2}. \quad (15)$$

If $f_t \ll f_g$, the effect is seen to be largely in quadrature, implying that the predominant effect of nonlinearity is to shift the phase of the transmission. In that case, the differential delay, defined here as $DD = -\Delta\varphi/\omega_t$, is

$$DD \approx \frac{-1}{2\pi f_g}\left[2r_2\frac{\tilde{f}_s}{f_g} + 3r_3\frac{\tilde{f}_s^2}{f_g^2}\right] \text{s}. \quad (16)$$

This is the form of the display on the link analyzer when $\tilde{f}_s$ represents the X coordinate.

To illustrate the magnitude of the effect, suppose $f_g = 50$ MHz, and that the only nonlinearity is that of the sinusoidal mixer curve. Let $\varphi_c = 0°$, and let $\tilde{f}_s$ vary ±10 MHz. For this case, $r_2 = 0$ and $r_3 = -1/6$. The differential delay, due to this third-order distortion term, is predicted to be 0.064 ns at either extreme of the sweep, and will show as a parabolic curve on the display. A finite value of r_2 will add a simple slope to the display.

C. Nonlinear Distortion and Intermodulation

Ramadan [8] has analyzed this problem for the injection-locked oscillator. The equations here are quite similar. For a phase-lock-loop receiver demodulator, Schilling and Smirlock [9] analyzed the intermodulation which appears at the output of the video amplifier when the device is used as a demodulator. The techniques used here closely follow [8], which has certain similarities to [9].

Adapting (8) to (4), the dynamic equation of the loop is

$$\frac{d\varphi_d}{dt} = 2\pi\tilde{f}_i - 2\pi f_g(\varphi_d + r_2\varphi_d^2 + r_3\varphi_d^3 \cdots). \quad (17)$$

Here it is assumed that f_g is real and uniform over the band of interest and that $\omega_m\tau_b \ll 1$. The first-order solution, neglecting r_2 and r_3, is taken as $\varphi_1(t)$. Let the second-order solution be

$$\varphi_d(t) = \varphi_1(t) + \varphi_2(t). \quad (18)$$

Substitution into (17) yields

$$\frac{d\varphi_2}{dt} = -2\pi f_g\{\varphi_2 + r_2(\varphi_1 + \varphi_2)^2 + r_3(\varphi_1 + \varphi_2)^3\}. \quad (19)$$

If $\varphi_2 \ll \varphi_1$, we may ignore cross-product and higher order terms in expanding (19), leaving the equation

$$\frac{d\varphi_2}{dt} = -2\pi f_g \varphi_2 - 2\pi f_g (r_2 {\varphi_1}^2 + r_3 {\varphi_1}^3). \quad (20)$$

Here, φ_1 being the known first-order solution, represents a driving function.

The first-order solution is given by (9). If $f_m \ll f_g$, this may be approximated as

$$\varphi_1 \approx \frac{f_i}{f_g}. \quad (21)$$

The term φ_2 represents distortion. Equation (20) has the same form as (17) taken to first order. Its solution is likewise approximated. The result, expressed as the distortion in frequency modulation, is

$$(\Delta \tilde{f})_{\text{distortion}} \simeq \frac{1}{2\pi} \frac{d}{dt} \left[-r_2 \left(\frac{\tilde{f}_i}{f_g} \right)^2 - r_3 \left(\frac{\tilde{f}_i}{f_g} \right)^3 \right]. \quad (22)$$

Following the methods of [6] and [7], we can estimate the effects of intermodulation in generating crosstalk noise in this amplifier. This is commonly measured in terms of the "noise power ratio" called NPR. In testing the system, a broad band of baseband noise is modulated onto the carrier. The input noise may or may not be removed from a narrow slot in this band by means of a band-reject filter. After transmission, intermodulation and other noise sources will reintroduce noise into the slot. The reintroduced noise is compared in level to the noise which is present when the input filter is absent. This ratio is the NPR. Following the approach of [7], the NPR, *due to intermodulation only*, is given by

$$\text{NPR}(f_m) = 10 \log \left[\frac{r_2^2 f_m^2 \tilde{f}_{\text{rms}}^2}{f_g^4} \left(2 - \frac{f_m}{f_{\max}} \right) + \frac{3 r_3^2 f_m^2 \tilde{f}_{\text{rms}}^4}{2 f_g^6} \left(3 - \frac{f_m^2}{f_{\max}^2} \right) \right] \quad (23)$$

where $\tilde{f}_{\text{rms}}$ is the rms deviation of the total band of noise, f_m is the frequency of the test slot, and $f_{\max}$ is the upper limit of the noise band being transmitted. In (23) the first term on the right represents second-order and the second term the third-order effects. In full system tests, the NPR usually includes other noise sources as well. Equation (23) does not include the effects of preemphasis, if used.

D. Effects of Amplitude Modulation

In saturated amplifiers of conventional types, variations in the input amplitude cause phase variations at the output. Because of imperfect limiting and other network parameters, the input signal reaching the power amplifier of an FM system may have undesired amplitude modulation of small depth in addition to the intended frequency modulation. Commonly, power amplifiers for this application are specified to have a maximum amplitude-to-phase conversion coefficient, expressed in degrees of phase change per decibel of amplitude change at the normal operating level. Such phase variations can introduce nonlinear distortion into the system, causing intermodulation among the baseband frequency components.

In the phase-lock system, the nonlinear effects induced by residual AM differ from those of a conventional saturated amplifier. The primary source of this distortion will be found in the mixer. Typically, a balanced mixer's response is given by an expression such as (2). If, at the carrier frequency, $\varphi_i - \varphi_o = \varphi_c = 0$, the error current is zero and the phase of the response is, to first order, independent of the input amplitude v_{ic}. However, if the system is tuned with a finite value of φ_e at the carrier frequency, φ_c, and there is no frequency modulation applied, we can determine the rate of change of phase as the input amplitude is varied *slowly*. In this situation, the frequency remains constant; therefore, i_e remains constant. Then

$$di_e = 0 = \frac{\partial i_e}{\partial v_c} dv_c + \frac{\partial i_e}{\partial \varphi_e} d\varphi_e \quad (24)$$

$$\Delta\varphi_e = -\frac{\Delta v_c}{v_c} \tan \varphi_c \quad (25)$$

$$\frac{\Delta\varphi_e}{\Delta(10 \log P_i)} \approx 6.5 \tan \varphi_c \text{ deg/dB}. \quad (26)$$

The previous equation is a *static* characterization. Tan φ_e is, typically, small compared with 1.0.

Dynamically, the effects of AM are somewhat more difficult to characterize. It might be assumed that there are amplitude changes which are correlated with the frequency deviation. These may occur in the input wave *or the output wave*, and either or both can introduce distortion. Depending upon the type of diodes used in the mixer and upon the relative power levels of the two applied signals, the mixer's sensitivity to amplitude changes may be quite different at the two ports, and should be determined by experimental study. Equation (2) is deduced by assuming that the diodes have square-law behavior. The following equations are based on (2) and are intended only to illustrate the nature of the problem. The relationship, in this case, *may apply to input AM, or output AM generated in the VCO by varactor modulation*, as it affects the mixer when fed back.

Again using a power-series representation, dimensionless modulation coefficients m_1 and m_2 may be used to characterize a linear and a quadratic relationship between the amplitude and the modulation deviation according to the equation

$$v_i = v_{ci} \left[1 + m_1 \frac{\tilde{f}(t)}{\tilde{f}_{d\max}} + m_2 \left(\frac{\tilde{f}(t)}{\tilde{f}_{d\max}} \right)^2 \right] \cos \varphi_i(t). \quad (27)$$

Here we simplify the problem by assuming that the video amplifier is linear and that the tuning curve of the oscillator is linear, and that there is no frequency offset between the carrier frequency and the oscillator so that $\varphi_c = 0$ and $\varphi_d = \varphi_e$. The previous equations imply that

$$i_e \approx k \left(1 + m_1 \frac{\tilde{f}}{\tilde{f}_{d\max}} + m_2 \left(\frac{\tilde{f}}{\tilde{f}_{d\max}} \right)^2 \cdots \right) \sin \varphi_e. \quad (28)$$

Noting that $\tilde{f} \simeq f_g \varphi_e$ and $\sin \varphi_e = \varphi_e - {\varphi_e}^3/6 \cdots$, we

obtain

$$i_e \approx k\left(1 + m_1 \frac{f_g}{\tilde{f}_{d\max}} \varphi_e + m_2 \left(\frac{f_g^2}{\tilde{f}_{d\max}^2}\right) \varphi_e^2\right)\left(\varphi_e - \frac{\varphi_e^3}{6} \cdots\right) \quad (29)$$

$$f_o = f_c + f_g(0)\left[\varphi_e + m_1 \frac{f_g}{\tilde{f}_{\max}} \varphi_e^2 + \left\{-\tfrac{1}{6} + m_2 \left(\frac{f_g^2}{\tilde{f}_{\max}^2}\right)\right\} \varphi_e^3 \cdots\right]. \quad (30)$$

This may be related to (4). This implies that a linear slope in the input RF voltage versus frequency curve has an effect similar to that of second-order nonlinearity in the $\varphi - f$ curve of Fig. 2. Similarly, a quadratic variation of amplitude versus frequency introduces third-order distortions. The effects may be evaluated by the methods of the previous section, by setting $r_2 = m_1 f_g/\tilde{f}_{\max}$, etc.

IV. FM Noise

A. Noise Arising in the Oscillator

The FM noise of a free-running diode oscillator is describable by the following equation, adapted from Kurokawa [10]

$$\overline{\Delta \tilde{f}_{\text{osc}}^2} = \frac{f_c^2 k_b T_d(f_m) B}{P_o Q_{\text{ext}}^2}. \quad (31)$$

This applies to an internally lossless singly tuned resonator which may contain one or more negative-resistance diodes. $T_d(f_m)$ is the "FM noise temperature" of the diode, arbitrarily defined by the equation[3]

$$T_d(f_m) = \frac{\overline{i_{n\varphi}^2}(f_c \pm f_m)}{4k_b |G_d| B} \quad (32)$$

where k_b is Boltzmann's constant, G_d is the effective negative conductance of the diode, and $\overline{i_{n\varphi}^2}$ is the noise-fluctuation current generated in the oscillating diodes in the frequency bands above and below the carrier frequency which are effective in frequency modulating the oscillator at the rate f_m.

If the noise currents $\overline{i_{n\varphi}^2}$ in (32) are shot-noise related, proportional to I_o as in the familiar shot-noise expression $\overline{i_n^2} = 2qI_oB$, the temperature T_d will not be a function of the size or number of diode chips used, inasmuch as the negative conductance G_d and the dc current I_o will both be proportional to the total cross-section area of the semiconductor wafer material. Equation (31), therefore, shows the dependence upon the total "optimum" power capability P_o and the external Q, where T_d is dependent upon the electrodynamic characteristics of the semiconductor wafer *material*. T_d is to be evaluated for an RF voltage excitation level which is "optimum" for the class of device used; that is, at a point where it is most efficient at generating power or where the best compromise is achieved between efficiency and signal-to-noise ratio. In high-level, efficient operation, the noise temperature T_d will usually be much greater than at low level, particularly in IMPATT diodes.

Under phase-lock conditions, the noise of (31) is suppressed by feedback by the factor $|K_s|^2$ from (11). At lower frequencies where f_g may be taken as real and excess delay may be neglected, the FM noise at the output, due to oscillator fluctuations, is given by the approximate formula

$$\Delta \tilde{f}_{\text{plo}}^2 = \frac{f_c^2 k_b T_d B}{P_o Q_{\text{ext}}^2} \frac{f_m^2}{f_m^2 + f_g^2}. \quad (33)$$

B. Noise Arising in the Mixer and Video Amplifier

If the mixer has a video source impedance of $Z_m\ \Omega$, with a real part R_m, and the video amplifier has an input impedance Z_a and a noise figure F_a under these input conditions, we may account for the amplifier noise by inserting a noise voltage generator at the input of value v_{amp}, giving an open-loop frequency deviation $\Delta \tilde{f}_{\text{amp}}$

$$\overline{v_{\text{amp}}^2} = 4k_b T_o B R_m (F_a - 1)$$

$$\overline{\Delta \tilde{f}_{\text{amp}}^2} = \frac{4k_b T_o B R_m}{|Z_m + Z_a|^2} |Z_{21} S|^2 (F_a - 1). \quad (34)$$

If the mixer diodes have an apparent noise temperature T_m with noise-free microwave inputs, their noise may be accounted for by another voltage generator of value v_{mix}, giving an open-loop frequency deviation $\Delta \tilde{f}_{\text{mix}}$

$$\overline{v_{\text{mix}}^2} = 4kT_m B R_m$$

$$\overline{\Delta \tilde{f}_{\text{mix}}^2} = \frac{4kT_m B R_m}{|Z_m + Z_a|^2} |Z_{21} S|^2. \quad (35)$$

C. Input Noise

When driven by two synchronized signals of zero phase difference, amplitude fluctuations of the microwave sources generate no noise in a balanced mixer. Phase fluctuations of the input signal generate current fluctuations according to (2). If the input signal is a noise-free carrier plus background thermal noise of temperature T_o, the apparent frequency modulation of the input is given [7] by

$$\overline{\Delta \tilde{f}_i^2} = \frac{f_m^2 k_b T_o B}{P_t}. \quad (36)$$

D. Total FM Noise and Noise Figure

Under closed-loop conditions, the noise from the mixer diodes, the video amplifier, and the oscillator are suppressed by the factor $|K_s|^2$. The input FM noise is transmitted by the factor $|T_{\text{fm}}|^2$. The total FM noise of the system is then

[3] The noise-current spectrum of an oscillating diode is not "white" and will involve correlations between components above and below the carrier frequency. Here, $\overline{i_{n\varphi}^2}(f_c \pm f_m)$ is taken to mean the effective spectral density as it affects the FM noise. The diode noise temperature T_d is an artificial but useful concept. The term "noise measure" (M) is sometimes used instead of temperature, where $M = T_d/T_o$, where $T_o \simeq 290$ K.

expressed as

$$\overline{\Delta \tilde{f}_o^2} = |T_{\text{fm}}|^2 \overline{\Delta \tilde{f}_i^2} + |K_s|^2 \{\overline{\Delta \tilde{f}_{\text{mix}}^2} + \overline{\Delta \tilde{f}_{\text{amp}}^2} + \overline{\Delta \tilde{f}_{\text{osc}}^2}\}. \quad (37)$$

For our purposes, the FM noise figure is defined by the following equation. This is the input signal-to-noise ratio divided by the output signal-to-noise ratio, as it affects the frequency modulation only.

$$F_{\text{fm}} = \frac{(\overline{\tilde{f}_d^2})_{\text{in}}}{(\overline{\tilde{f}_d^2})_{\text{out}}} \left(\frac{\overline{\Delta \tilde{f}_o^2}}{\overline{\Delta \tilde{f}_i^2}} \right). \quad (38)$$

Equation (38) may be expressed in simple and familiar terms by substituting (36), (37) and an expression for P_i, involving the factor k from (5), and the available gain of the mixer G_m. The available gain, if the mixer were to be used in a superheterodyne receiver, where the input signal and the local oscillator differ by the frequency f_m, is given by the ratio of the *available* output IF power to the input signal power P_i, when the IF load impedance is conjugately matched to the mixer impedance. For this case, the available gain is given by

$$G_m = \frac{k^2 |Z_a + Z_m|^2}{8 R_m P_i} \quad (39)$$

and the FM noise-figure expression becomes

$$F_{\text{fm}} = 1 + \frac{F_a - 1 + \dfrac{T_m}{T_o}}{2G_m} + \frac{P_i}{P_o} \frac{T_d}{T_o} \frac{f_c^2}{f_g^2} \frac{1}{Q_{\text{ext}}^2}. \quad (40)$$

The divisor of 2 in the second term appears because the input thermal noise bandwidth is twice that of the video amplifier.

The diode noise temperature T_d must be determined in order to evaluate this expression. It is not commonly provided on diode data sheets, nor are there quantitatively meaningful theories applicable for Gunn and IMPATT diodes under high-level oscillator conditions. Useful values are best obtained by experiment. If the diode type to be used has been tested in any "good" free-running oscillator circuit where Q_{ext} is known, (31) can be applied to determine the value of T_d applicable to that diode. Some typical values for T_d/T_o are $\sim 10^5$ for silicon IMPATT diodes and ~ 500 for Gunn diodes operating in the 10–12-GHz range, for video frequencies in the range 1–10 MHz.

V. Comparison with Reflection Amplifiers

A. Gain and Bandwidth Discussion

At present, for frequencies of ~ 6 GHz and above, most solid-state power amplifiers are of multistage design using IMPATT or Gunn negative-resistance diodes in circulator-coupled reflection circuitry [1], [2]. Some use stable "linear" amplifier stages while others use injection-locked oscillator stages. Very large bandwidth is possible with stable devices, up to several hundred megahertz, but the gain per stage is low. Higher gain per stage is possible with injection-locked oscillators, with reduced bandwidth. With VCO phase-lock, the gain of a single stage may be much greater still, sufficient for many power-amplifier applications in radio-relay communications, with adequate bandwidth for most microwave FM communications systems.

The equations for the dynamic response in FM service for the injection-locked device are quite similar to those for the VCO phase-lock device, and a direct comparison is instructive. In both cases, we define a "characteristic frequency" f_g ,which is the critical parameter governing the locking range, the usable bandwidth, noise suppression, and linearity. A large value for f_g is desirable.

To a first approximation, f_g is one-half the locking range in either case. For the injection-locked oscillator (ilo), Adler's theory as presented in [11] may be modified to give the expression

$$(f_g)_{\text{ilo}} = \frac{f_c}{Q_{\text{ext}} \sqrt{G}} \quad (41)$$

where G is the power gain. We have presented the expression for the VCO phase-locked oscillator (plo) in (6)

$$(f_g)_{\text{plo}} = k Z_{21}(\omega_m) S. \quad (6)$$

One significant difference is that f_g in (41) is usually real and constant, while in (6) it is a complex function of the modulating frequency ω_m. The dynamic equations (9)–(11) apply equally well to either device [12], [8] if the feedback delay is neglected. The suppression of nonlinear distortion also follows similar equations [8], although there are additional sources of nonlinearity in the VCO approach. For purposes of comparison and discussion, we may assume that the system requirements are equivalent for the two devices, requiring equal values for f_g and gain.

In (41) the maximum gain is determined by Q and f_g, and for most applications, it is insufficient to meet the system requirements in a single stage. In (6), however, the locking effect is enhanced by the gain of the video amplifier in combination with phase detection and varactor tuning, so that much higher gain may be obtained for the same value of f_g. This will be sufficient, in many cases, to allow use of a single phase-lock stage.

No attempt has been made to determine the ultimate limitations on gain and bandwidth in a figure-of-merit type of equation for the VCO phase-lock approach. Such limitations exist, nevertheless, and are ultimately imposed by considerations of stability. If one wishes to increase the gain substantially be reducing the input power, the factor k in (6) will be reduced correspondingly. To maintain a constant value for f_g, the gain Z_{21} must be increased. This will increase the delay in the amplifier, reducing the stability margin and increasing the gain-peaking effects illustrated in Fig. 4. As indicated earlier, loop delay is a critical parameter. Further study is needed to determine the optimum frequency-response characteristic for the function f_g using standard methods of feedback system design.

B. Noise Comparison

For a free-running oscillator, the FM noise is given by (31). When phase locked by *either* approach the noise of a

single device is reduced to the same expression of (33). This might imply equivalence. However, to maximize the gain and/or bandwidth, an injection-locked device is typically designed for minimum Q. For a VCO phase-locked device, a higher Q oscillator may be used intentionally, in order to reduce the noise. Also, the injection-locked device will usually require additional stages and their contributions must also be included.

It is more instructive to compare the complete expressions for the FM noise in both cases, including the mixer and video amplifier for the VCO device and the earlier stages for the injection-locked device.

In (42)–(46a) we present certain noise expressions for a multistage reflection amplifier, based upon linear theory with an assumption of distortion-free amplification. For a single-stage amplifier, the noise figure is related to the gain and the temperature (or the noise measure) by the well-known expression

$$F = 1 + \frac{T_d}{T_o}\left(1 - \frac{1}{\text{Gain}}\right). \tag{42}$$

The expression for a tandem multistage device with gains G_1, G_2, etc., and noise figures F_1, F_2, etc., is given by

$$F_{\text{tot}} = F_1 + \frac{F_2 - 1}{G_1} + \frac{F_3 - 1}{G_1 G_2} \cdots \frac{F_n - 1}{G_1 G_2 \cdots G_{n+1}}. \tag{43}$$

The output FM noise is given by (44), based upon (36) and (38)

$$\overline{\Delta f_{\text{out}}^2} = \overline{\Delta f_i^2} + (F_{\text{tot}} - 1)G_{\text{tot}}\frac{f_m^2 k_b T_o B}{P_o} \tag{44}$$

where $\overline{\Delta f_i^2}$ is the input noise deviation. Substituting (42) into (43) and then into (44) we obtain the overall expression for the FM noise output of a multistage reflection amplifier where the diode noise temperatures of the stages are $T_1, T_2, \cdots, T_n$.

$$\overline{\Delta f^2} = \overline{\Delta f_i^2} + \frac{f_m^2 k_b T_o B}{P_o}\left[\frac{T_1}{T_o}(G_1 - 1)(G_2 G_3 \cdots G_n) + \frac{T_2}{T_o}(G_2 - 1)(G_3 G_4 \cdots G_n) \cdots + \frac{T_n}{T_o}(G_n - 1)\right]. \tag{45}$$

For purposes of comparison, it is next assumed that the multistage reflection amplifier is separable into two sections, a low-noise preamplifier of one or more stages using one class of diodes with noise temperature T_a and a combined gain G_a, followed by a power-amplifier section of one or more stages using noisy diodes of temperature T_d and a combined gain of G_d. The first equation in (46) gives the noise deviation for this device. The second equation of (46) is obtained by substituting (40) into (44), giving the noise deviation for the VCO phase-lock device.

$$(\overline{\Delta f^2})_{\text{ref}} = \overline{\Delta f_i^2} + \frac{f_m^2 k_b T_o B}{P_o}\left[\frac{T_a}{T_o}(G_a - 1)G_d + \frac{T_d}{T_o}(G_d - 1)\right] \tag{46a}$$

$$(\overline{\Delta f^2})_{\text{plo}} = \overline{\Delta f_i^2} + \frac{f_m^2 k_b T_o B}{P_o}\left[\frac{\left(F_a - 1 + \frac{T_m}{T_o}\right)G_a G_d}{2G_m} + \frac{T_d}{T_o}\frac{f_c^2}{f_g^2 Q_{\text{ext}}^2}\right]. \tag{46b}$$

In each bracketed expression on the right, the second term represents the noise contribution of the power output stage or stages which use noisy diodes of temperature T_d. The first expression in the brackets of the first equation is the contribution of all low-noise preamplifier stages, and in the second equation it is the contribution of the mixer and video amplifier combination.

If we now compare (46a) and (46b) we see that the VCO phase-lock device is *equivalent* to a low-noise preamplifier of high gain followed by a noisy post-amplifier, in the same manner as in (46a). Here the "equivalent gain" of the power (VCO) stage is given as

$$G_{\text{VCO}} = 1 + \frac{f_c^2}{Q^2 f_g^2}$$

and the noise figure of that stage is approximately equal to the "noise measure" of the diode, T_d/T_o. The remainder of the microwave gain may be ascribed to the electronic circuitry of the mixer and video amplifier, with their combined noise figure. For example, if $f_g = 50$ MHz, $f_c = 11$ GHz and $Q = 100$, then $G_{\text{VCO}} = 7.7$ dB. For our computed example in Section VI, the total gain is 34 dB and that assigned to the mixer plus video amplifier is 26.3 dB.

Observe that the noise contribution from the power diodes in a reflection amplifier will exceed that from the VCO in the phase-lock amplifier if *the total gain which they alone provide* exceeds the "equivalent gain" of the VCO, G_{VCO}.[4] Furthermore, the noise contributions from the preamplifier stages in the reflection amplifier will exceed that from the mixer and video amplifier in the phase-lock amplifier unless their effective noise figure is comparable or better.

VI. Sample Computations

For purposes of illustration, sample computations are presented here for the basic characteristics of a phase-lock-loop amplifier using a set of assumed component parameters. The assigned values are believed to be achievable with existing technology.

1) $f_g(0) = 50$ MHz/rad (achieved).
2) $f_{co} = 300$ MHz (achieved).
3) $T_d = 10^5 \times T_o$, ($M = 50$ dB) (typical).
4) $T_m = 600$ K (arbitrarily assigned).
5) $P_o = 5$ W (assumed).
6) $P_i = 0.002$ W (assumed).
7) $Q_{\text{ext}} = 100$ (achieved).
8) $r_2 = -0.05$ (arbitrarily assigned).
9) $r_3 = -0.2$ (arbitrarily assigned).
10) $m_1 = -0.02$ (0.35-dB change for 20 MHz, arbitrarily assigned).

[4] Equating the last term of (46a) with (46b).

11) $m_2 = -0.01$ (+0.08-dB change at ± 10 MHz, arbitrarily assigned).
12) $\tilde{f}_{\max} = \pm 10$ MHz [maximum deviation for 10) and 11)].
13) $G_m = -6$ dB (conversion loss of mixer, arbitrarily assigned).
14) $F_a = 6$ dB (video amp NF @ 8 MHz, arbitrarily assigned).
15) $f_{\max} = 8$ MHz (noise-loading bandwidth).
16) $\tilde{f}_{\text{rms}} = 1.0$ MHz (noise-loading deviation).
17) $f_m = 8$ MHz (top channel for NPR calculation).

The computations are summarized as follows.

1) Frequency response, see Fig. 3.
2) Noise figure [(40)] 23.3 dB.
3) Differential delay [(16)]:
   a) from r_2, slope ± 0.063 ns @ ± 10 MHz;
   b) from r_3, parabolic $+0.08$ ns @ ± 10 MHz;
   c) from m_1 slope ± 0.127 ns @ ± 10 MHz;
   d) from m_2, parabolic $+0.159$ ns @ ± 10 MHz.
4) Intermodulation NPR, combining effects of a), b), c), and d), from (23).
   a) effective value of $r_2 = -0.05 - 0.1 = -0.15$;
   b) effective value of $r_3 = -0.2 - 0.25 = -0.45$;
   c) 2nd-order NPR $= -66.5$ dB;
   d) 3rd-order NPR $\doteq -86$ dB.
5) Fm noise deviation in a 3.1-kHz-wide channel at 8.0 MHz, induced by phase-lock amplifier only.

$$\overline{\Delta \tilde{f}^2} = \frac{F_{\text{fm}} f_m^2 k_b T_o B}{P_i} = 83 \text{ Hz}^2$$

$$\Delta \tilde{f}_{\text{rms}} = 9.15 \text{ Hz}.$$

Compared with test tone $\tilde{f}_{tt} = 140$-kHz rms

$$10 \log \frac{\overline{\Delta \tilde{f}^2}}{\tilde{f}_{tt}^2} = -83 \text{ dB}.$$

VII. Experimental Results

An experimental phase-lock system has been built and tested. The device operates in the 10.7–11.7-GHz band. Two versions have been used. In one, a Gunn VCO was used, giving a power output of 250 mW when driven by a 3-mW input. In the second version, an output of 3 W was obtained using two IMPATT diodes in a Kurokawa-type oscillator [8]. Both were tuned with a single varactor.

The Gunn-effect device has a locking range of ~ 110 MHz. With a variable input frequency, acquisition of lock occurs at the same band edges when approached from outside the band. A lockup search routine is neither necessary nor desirable. Over the 10.7–11.7 band, single-knob tuning is sufficient and no instrumentation is needed except a voltmeter to observe the average varactor bias level.

Extensive tests of the Gunn device were conducted in the laboratory of a major manufacturer of communications equipment. Frequency-response tests showed negligible variation in the response of the frequency modulation over the 0–8-MHz range. Link-analyzer data are shown in Fig. 6. The upper two curves show differential gain, with the same data on each curve. The separation of the two curves is a calibration method, representing 1.0-percent departure from linearity. The lower two curves present differential delay data for a test tone at 555 kHz. The curve separation here represents 1.0 ns. It is seen that differential gain over the ± 22-MHz range is not more than ~ 0.25 percent and that the delay variation is no greater than ~ 0.25 ns over a range $-22 < \tilde{f}_s < +12$ MHz. A second set of curves shows the effect of reducing the input power by 6 dB.

In the noise-loading test to determine the NPR, the background NPR of the transmitter and receiver used in the test exceeded that of the phase-lock amplifier. The system was noise loaded for 1800 channels with a CCIR standard signal with the recommended preemphasis. The background NPR values varied from 52.5 to 54 dB in the various frequency slots. Addition of the Gunn-diode phase-lock device degraded this to the range 51–53 dB, implying that its NPR was in the general range of 58 dB. The "idle" noise test without noise loading had a background level of ~ 55 dB which was degraded by about 1 dB. This implies a noise figure on the order of 29 dB.

The 3-W IMPATT device is a preliminary model made by adapting another oscillator into a VCO. The test shows feasibility of the principle. The device is believed to be suitable for television relay, but its noise level and linearity are not adequate for FDM multiplex service. The Q was only 40, f_g was estimated to be 20 MHz/rad, and a 5-mW input signal was used. Link-analyzer data for ± 10 MHz are shown in Fig. 7. The noise figure was measured and found to be ~ 39 dB. Theoretical expectation based upon (40) is 45 dB, assuming $T_d/T_o = 10^5$.

VIII. Conclusions

It has been demonstrated experimentally that a phase-lock loop can serve as a power amplifier for microwave FM communications signals. Theoretical relationships have been provided which show the relationships between the internal parameters and the performance of the system as an amplifier.

Acknowledgment

The authors wish to thank the numerous people at Microwave Associates who have contributed to this effort, in helpful advice, and in providing special components and subassemblies. They also wish to thank R. Rearwin, F. Collins, J. Fackler, P. Setzco, and R. Urlau.

References

[1] *IEEE Trans. S-MTT, Special issue on Solid State Microwave Power Amplifiers*, vol. MTT-21, no. 11, entire issue, Nov. 1973.
[2] I. Tatsuguchi and J. Gewartowski, "A 10-watt 6-GHz GaAs IMPATT amplifier for microwave radio systems," *Int. Solid-State Circuits Conf. Digest of Papers*, IEEE Cat. No. 73 CHO 711-2 ISSCC 1975, pp. 134–135.
[3] S. C. Gupta, "Phase locked loops," *Proc. IEEE*, vol. 63, no. 2, pp. 291–306, Feb. 1975.
[4] J. Klapper and J. J. Frankle, *Phase-Locked and Frequency Feedback Systems*. New York: Academic Press, 1972.
[5] P. G. Debois and G. Quaghebeur, "8 watts 6 GHz 1800 channel all-solid-state radio relay transmitter," *Proc. 3rd EuMC*, Brussels 1973, paper B.12.2.
[6] J. Salmon, "A MIC phase-locked-loop avalanche oscillator in X-band," *IEEE Trans. S-MTT*, vol. 22, no. 4, p. 464, April 1974.
[7] Bell Tel. Labs. Tech. Staff, *Transmission Systems for Communica-*

tions, pub. by Bell Tel. Labs. Inc., Fourth Edition, December 1971, Ch. 10.
[8] M. Ramadan, "Intermodulation distortion of FDM-FM in injection-locked oscillator," *IEEE Trans. Comm.*, vol. COM-21, no. 3, pp. 191–194, March 1973.
[9] D. L. Schilling and M. Smirlock, "Intermodulation distortion of a phase-locked loop demodulator," *IEEE Trans COM*, vol. 15, pp. 222–228, Apr. 1967.
[10] K. Kurokawa, "Tne single-cavity multiple-device oscillator," *IEEE Trans. Microwave Theory Tech.*, vol. MTT-19, pp. 793–801, October 1971.
[11] M. E. Hines, "Negative resistance diode power amplification," *IEEE Trans. Electron Devices*, vol. ED-17, Jan. 1970 [see eq. (24)].
[12] M. E. Hines, J. C. Collinet, and J. G. Ondria, "FM noise suppression of an injection-locked oscillator," *IEEE Trans. Microwave Theory Tech.*, vol. MTT-16, pp. 738–742, September 1968, [see eq. (33)].
[13] F. M. Gardner, *Phaselock Techniques*. New York: John Wiley Publications, 1966.

Propagation of Cladded Inhomogeneous Dielectric Waveguides

MASAHIRO HASHIMOTO, MEMBER, IEEE

Abstract—**An approximate theory on the propagation of modes in an arbitrarily inhomogeneous optical waveguide embedded in a homogeneous medium is presented. Simple formulas are given, whereby the propagation constants can be determined assuming that the analytic solution is known in the absence of cladding. The results obtained applying the theory to a truncated parabolic-index profile are shown to be in good agreement with those obtained by the rigorous analysis. The theory is also applied to the propagation of TE and TM waves in truncated near-parabolic-index media.**

Introduction

An important aspect of guided waves propagating in inhomogeneous (graded) index dielectric waveguides involves the investigation of the propagation characteristics subjected to signal distortion. Recently, considerable effort has been expended to compute the propagation constants of modes by means of high-accuracy straightforward computation [1], because it is very difficult to obtain an analytic solution except for a certain index profile. The analytic approach becomes more difficult for the cladded inhomogeneous dielectric waveguide in which the graded-index medium is suspended in a homogeneous medium.

In a recent work [2], the purely mathematical techniques, based on the integral representation of a solution of Hermite's differential equation, have successfully been applied to a cladded parabolic-index waveguide, and the mode functions have been obtained in analytic form.

Manuscript received October 17, 1975; revised January 13, 1976.
The author was with the Communication Research and Development Department, Communication Equipment Works, Mitsubishi Electric Corporation, 80 Nakano, Amagasaki 661, Japan. He is now with the Department of Applied Electronic Engineering, Osaka Electro-Communication University, Neyagawa, Osaka 572, Japan.

The aim of this paper is to develop an approximate theory of propagating modes in a general class of cladded inhomogeneous dielectric waveguides. This theory is verified by comparing the results with those obtained exactly in a case of parabolic-index profile.

We here consider the two-dimensional waveguide in which the refractive index varies in the transverse x direction as (see Fig. 1)

$$n(x) = \begin{cases} n_0\sqrt{1-\chi(x)}, & \text{for } |x| < x_c \\ n_0\sqrt{1-\chi(x_c)}, & \text{for } |x| > x_c \end{cases} \quad (1)$$

where $\chi(x)$ is an even and a smooth function satisfying $\chi(0) = 0$ (see Fig. 1), and n_0 is the refractive index at the center axis z ($x = 0$). The lower order modes are allowed to propagate along the z axis in the guiding medium $|x| < x_c$, and the undesirable higher order modes are radiated through the homogeneous outer medium $|x| > x_c$. The present approximate theory is developed for the TE wave propagation along such a waveguide. However, it is shown that the theory can be extended to the problem of the TM wave propagation. An example of determining the propagation constants of TM waves in truncated near-parabolic-index media is given in the last subsection.

Modes in an Ideal Waveguide

The starting point is the knowledge of modes (electric-field functions), including propagation constants, in the ideal waveguide, which is defined as an uncladded waveguide consisting only of the guiding material (the index distribution is indicated by the dotted curve in Fig. 1).